

March 1993  
(A)

## MODELING ACCELERATOR STRUCTURES AND RF COMPONENTS\*

K. Ko, C.-K. Ng and W. B. Herrmannsfeldt  
Stanford Linear Accelerator Center  
Stanford University, Stanford, CA 94309

## ABSTRACT

Computer modeling has become an integral part of the design and analysis of accelerator structures and RF components. Sophisticated 3D codes, powerful workstations and timely theory support all contributed to this development. We will describe our modeling experience with these resources and discuss their impact on ongoing work at SLAC. Specific examples from R&D on a future linear collider and a proposed  $e^+e^-$  storage ring will be included.

## 1. INTRODUCTION

There has been a dramatic increase in computer modeling at SLAC due to the R&D on two future accelerators: the Next Linear Collider (NLC) [1] and the Asymmetric B Factory based on PEP (PEP-II) [2]. This is particularly evident in the modeling of accelerator structures and RF components in three dimensions. A test accelerator (NLCTA) [3] is presently under construction and one of its goals is to integrate the new technologies of the X-band RF system (klystron, pulse compression, linac structure) being developed for a TeV scale NLC into a fully engineered sector. For PEP-II, a high power test cavity with a novel higher-order mode (HOM) damping scheme [4] is to be constructed to study its electrical and mechanical performance under operating conditions at high currents. At the moment a substantial modeling effort is devoted to the design and analysis of the many complex cavities and structures involved in these two projects.

Most RF structures in an accelerating system possess geometrical symmetries which allow them to be treated by two-dimensional programs or even by analytical means. There are, however, critical components that are non-symmetrical for which three-dimensional modeling is needed. Previously, the engineering of such components would require repetitive prototyping and cold testing. At SLAC we are making a concerted effort to minimize these time consuming and costly experimental procedures and to move towards nondestructive testing by computer modeling. This alternative approach would not have been feasible without several major developments in modeling resources. They include advances in 3D programs, the speedup in affordable CPU's, and timely theory support. We will discuss each of these resources in the next section.

## 2. MODELING RESOURCES

*(i) 3D Codes*

Computer programs to model cylindrically symmetric RF structures have been in routine use for over a decade in accelerator and power tube research. A prime example is SUPERFISH [5] for finding monopole modes in axisymmetric structures. Truly three-dimensional codes for non-axisymmetric structures made their appearances more recently and are just beginning to gain widespread use. A more detailed discussion on 3D RF cavity codes has been presented elsewhere [6]. Here we will only summarize as follows.

Presently available codes are either based on a finite-difference (FD) (Fig. 1a) or finite-element (FE) mesh (Fig. 1b). They can simulate cavity properties in the time and/or frequency domain (td or fd). Several of them also have the particle-in-cell (pic) option to include beam effects self-consistently. Two advances of interest to accelerator design are the quasi-periodic boundary condition for periodic structures and the S-matrix calculation for traveling wave structures. We list below several 3D codes which SLAC has had experience with. Structured on a FD mesh are:

---

\* Work supported by Department of Energy, contract DE-AC03-76SF00515.

- (a) MAFIA (*CST/Darmstadt*) - td with pic, fd,
- (b) ARGUS (*SAIC*) - td with pic, fd,
- (c) SOS (*MRC*) - td with pic, fd;

and on a FE mesh are:

- (d) HFSS (*HP/ANSOFT*) - fd,
- (e) EMAS (*MSC*) - td, fd,
- (f) ANTIGONE (*LAL/Orsay*) - td with pic, fd.

The FE codes have an automatic mesh-generator, model geometries better and can interface directly with thermal codes which are also FE based. The FD codes, on the other hand, have enjoyed a much longer lead time in implementation for RF applications. MAFIA [5], in fact, has its origin in the accelerator community; therefore it is not surprising that this set of codes offers the broadest range of capabilities related to accelerator design. ARGUS [5] is under further development for accelerator applications and is available to the community at large through the Los Alamos Accelerator Code Group (LAACG). SOS [5] is similar to MAFIA and ARGUS but is more oriented towards the simulation of microwave devices. Of the FE codes, HFSS [5] is probably the most widely known for S-matrix calculations. EMAS [5] has thus far attracted few users and we are just beginning to take a closer look at ANTIGONE [5]. At present MAFIA and HFSS are our standard programs for modeling cavities and structures although we are always receptive to any code that could provide better results on a specific design.

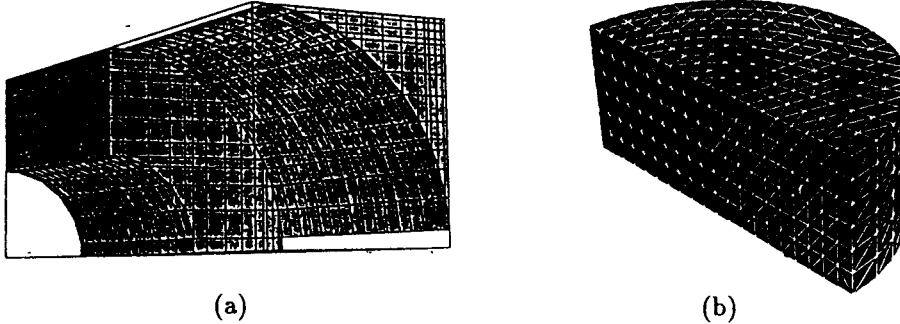


Fig. 1 (a) MAFIA finite-difference mesh and (b) ANTIGONE finite-element mesh.

### (ii) Computing Environment

3D modeling used to be considered practical only on supercomputers because of the long run time and large memory it requires. This is no longer the case as the workstation has become competitive in performance. For example, an IBM RISC 6000 model 580 processes at over 40 MFLOPs, allows up to 1024 MB RAM, and provides several GB of disk storage. These specifications come at a small fraction of the cost of a supercomputer. On such a machine with 512MB of RAM, we have modeled one half of the PEP-II RF cavity using MAFIA and calculated forty eigenmodes on a mesh with three-quarter of a million cells in less than 6 hours. This quick turnaround in actual clock time is important as it may translate into shorter design cycle and hence improved efficiency. A mainframe supercomputer is not likely to operate in a dedicated mode on a job to give fast turnaround at a sustained level. In terms of visualization, the workstation has powerful graphics which makes it ideal for 3D modeling since most of the effort involved is in geometry setup of the structure, and post-processing of the results.

Looking at the cost-differential, the effective performance and the open system/graphics advantage, the argument is rather convincing that the workstation could be a viable alternative to the supercomputer. Faced with limited cpu allocation from supercomputers and increasing modeling demand from NLC and PEP-II, we made the choice to go with 3D codes such as MAFIA and HFSS which had support for running on workstations. Today we have built a respectable network of workstations with sufficient computing power and memory to handle reasonably complex structures with relative ease.

### *(iii) Theory Support*

Although great progress has been made with 3D codes there are instances where they are limited in their capabilities. Many cavities in an RF system are coupled to external waveguides for power input or output, such as the input coupler to a linac or the output circuit of a klystron. Recently there has also been strong interest in HOM damping in accelerator cavities using waveguides. Therefore it is of great interest to know the resonant properties like frequency and external Q in such geometries. But this requires a matched load at the end of the waveguide which numerically is not possible since existing codes calculate real eigenfrequencies.

While the waveguide-loading effect on the cavity cannot be evaluated directly, the following theoretical methods have been successfully implemented to find external Q's from closed cavity data (real frequencies) computed with shorting planes as waveguide terminations:

- (1) Kroll-Yu/Kroll-Lin methods - find resonant frequency and external Q,
- (2) Kroll-Kim-Yu method - calculates S matrix of N-port cavities,
- (3) Arcioni method - produces an impedance versus frequency spectrum.

The Kroll-Yu method [7] requires four shorting plane positions in the waveguide to parametrize the resonance which is a complex frequency. Kroll-Lin [8] achieves the same result with two waveguide lengths but needs information about the field amplitudes at the shorting planes as well as the stored energies. For cavities with more than one port, the Kroll-Kim-Yu [9] method derives the S matrix at the frequency points where computer results are obtained. Normally several well chosen waveguide lengths are needed. In contrast, a single length is sufficient for the Arcioni method [10] to produce an impedance spectrum from which the resonant parameters can be deduced. However, modes with frequencies up to 1.5 times the frequency range of interest have to be taken into account for good accuracies. We have applied the Kroll-Yu/Kroll-Lin methods to a wide range of cavities with considerable success. The Kroll-Kim-Yu method is being tried out on some simple components and the results look very encouraging. Arcioni's method has seen limited application so far but an effort is ongoing to explore its potential further. Our experience is that when a direct numerical method is lacking, one can turn to an indirect method that combines theory with existing code capability.

### 3. MODELING EMPHASIS AND APPROACH

Up to now our 3D efforts on the workstations have focussed primarily on the cold tests of cavities and structures with no beams. The addition of particles vastly increases the complexity of the simulation and quickly pushes the limit of the hardware. We are continuing to work towards a hot test (e.g. klystron interaction), although any meaningful quantitative results will probably have to wait till the next jump in computing power and further code improvements. Meanwhile there is a lot to be learned from modeling cold tests and for most structures, the simulation has proven to be invaluable for design and analysis.

Our cold test modeling emphasizes the following: we require that the geometry be realistic, that is, the mesh reproduces closely the actual dimensions of the structure. We make certain that the simulation is physical; for example, proper boundary conditions are included. And we benchmark the model against established experimental data. These are essential steps to work through before one should consider doing serious design studies with the model.

Numerical cold tests can be performed either in the frequency or time domain. For normal mode analysis of cavities and periodic structures, we consider the time-harmonic solutions at steady-state and find the eigenfrequencies and eigenfunctions of the system. The quasi-periodic boundary condition allows arbitrary phase advance across a single cell in an infinite periodic chain. In waveguide-loaded cavities, theoretical methods described earlier make use of normal mode to produce external Q's. For transmission calculations of traveling structures, we solve for the time response due to a single-frequency externally driven field. Radiating boundary conditions permit power to be input and output through port boundaries at which the S matrix can be determined when steady-state is reached. In certain cases, the transient fields are of interest. Interestingly, HFSS evaluates the S matrix in the frequency domain.

#### 4. THREE-DIMENSIONAL RF STRUCTURES

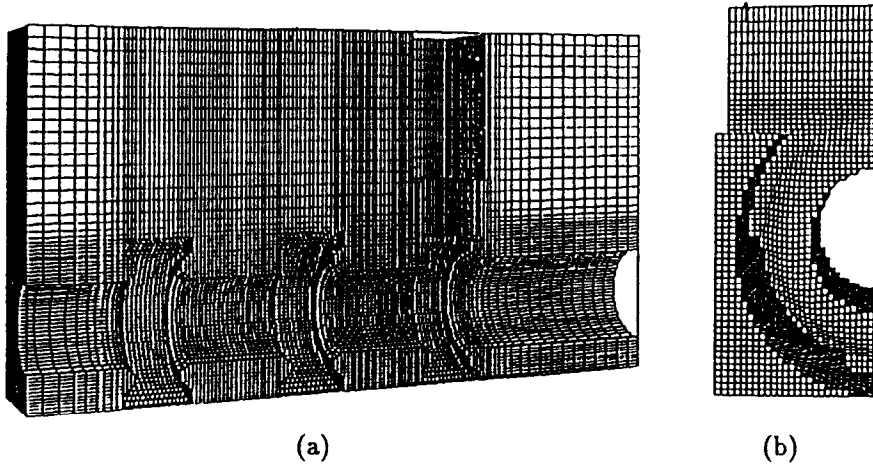


Fig. 2 (a) ARGUS model of klystron output cavity and (b) coupling slot between gaps.

In an RF structure, 3D effects can arise either intrinsically or due to external coupling. We will illustrate this by the 3-gap klystron output cavity shown in Fig. 2a. Even in the absence of the external waveguide, the cavity is intrinsically 3D because of the coupling slots in the common wall between the gaps (Fig. 2b). It is a standing wave cavity and the modes have zero group velocities because the cavity is closed. To extract power, the last gap is coupled to an external waveguide, hence making it a waveguide-loaded cavity. This causes the modes to have non-vanishing group velocities which is necessary for power flow to the waveguide. Strictly speaking the output circuit is no longer a standing wave cavity. The parameters that characterize the circuit are the frequency, the R/Q and the loaded Q or  $Q_L$  which is given by

$$\frac{1}{Q_L} = \frac{1}{Q_o} + \frac{1}{Q_e} \quad (1)$$

where  $Q_o$  is due to wall loss and  $Q_e$  is due to waveguide loading. In a closed or standing wave cavity  $Q_L$  is simply  $Q_o$  since  $Q_e$  is infinite. In a waveguide-loaded cavity,  $Q_L$  can have both contributions if the coupling is weak while for strong coupling, it is dominated by the waveguide loading and  $Q_L$  is just  $Q_e$ .

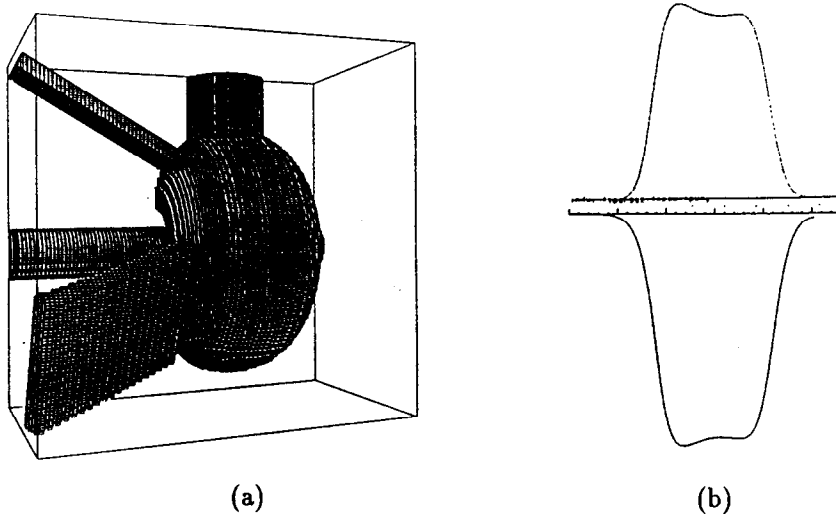
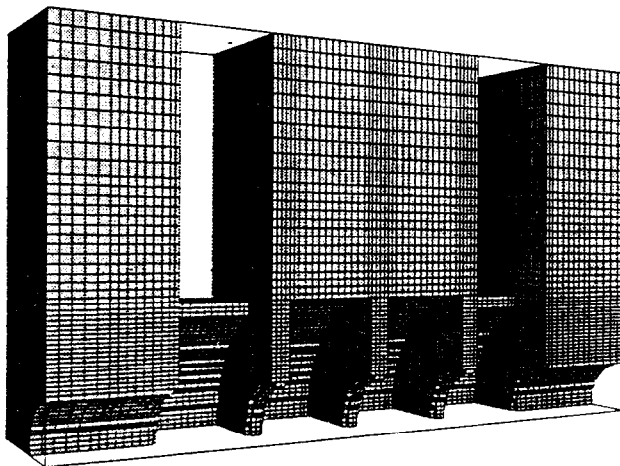


Fig. 3 (a) MAFIA model of PEP-II HOM damped RF cavity and (b) axial longitudinal field from measurement(top) and MAFIA(bottom).

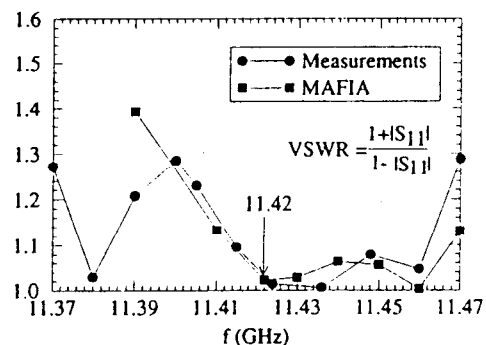
There are two types of modes in waveguide-loaded cavities such as the klystron output cavity of Fig. 2 or the PEP-II RF cavity shown in Fig. 3a. If their frequencies are below the waveguide cutoff then the modes are trapped as standing waves with high  $Q$ 's. Trapped modes are to be avoided in the klystron output circuit because they can be potentially harmful oscillations. The accelerating mode should ideally be the only trapped mode in the PEP-II cavity and the waveguides are designed not to degrade its shunt impedance appreciably. For trapped modes, standard eigensolutions would suffice provided the waveguides are sufficiently long.

When their frequencies are above the waveguide cutoff, the modes are untrapped and depending on the coupling, their  $Q$ 's can be moderately to very low. In a klystron output, low  $Q$ 's are desirable for all the modes but especially for the operating mode to transfer power out efficiently. In the PEP-II cavity, the untrapped modes are the HOM's that are targeted for damping and low  $Q$ 's are effective in reducing beam instabilities. The theoretical methods described in Section 2 are needed to evaluate the properties of these untrapped modes.

3D RF structures can also be of the traveling wave type. Figure 4a shows a short section of a disk-loaded waveguide with coupler cavities for power input and output. Without the couplers, the linac structure itself is described by the  $\omega - \beta$  diagram which can be generated using 2D codes and gives the traveling modes in a periodic structure of infinite extent. The couplers are necessarily 3D for power coupling away from the beam and for this, the 3D time-domain S-matrix calculation we mentioned earlier is required.



(a)



(b)

Fig. 4 (a) MAFIA model of NLCTA structure with input/output couplers and (b) VSWR vs. frequency of coupler from MAFIA and measurements.

## 5. MODELING RESULTS

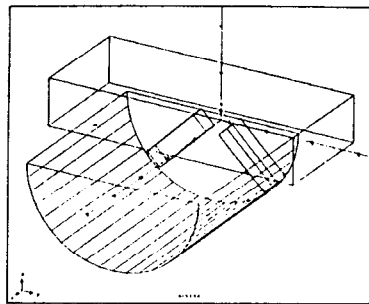
### (i) NLCTA RF System

The NLCTA RF system comprises the klystron, the pulse compression, and the linac all operating at 11.424 GHz. We will show examples of the crucial 3D components from each. For the klystron, the desired peak power (50 MW) and pulse length (1.5  $\mu\text{sec}$ ) pose a design challenge on the the output circuit to achieve high efficiency and to avoid gap breakdown. The ongoing approach is to raise the efficiency while lowering the gap voltage through extended interaction in the form of multi-gap structures. Many extended interaction circuits have been tested with varying degree of success. The 3-gap cavity in Fig. 2a was a design for which a cold test comparison was made between experiment and simulation [11]. Table 1 shows good agreement between the two results. The model also indicates uneven gap voltages and large field asymmetries which are undesirable. Consequently, the circuit was not put through hot tests, thus saving valuable time and resources.

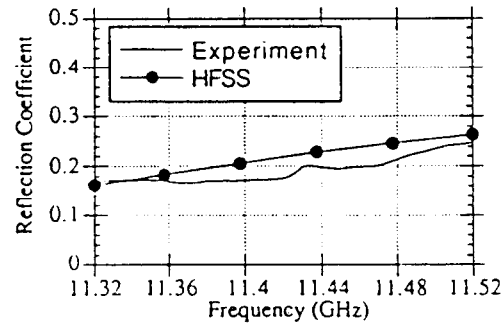
	$\pi$	$2\pi/3$	$2\pi$
Measured	10.07 (47)	10.40 (45)	11.54 (19)
Calculated	10.05 (45)	10.33 (44)	11.53 (20)

Table 1. Cold test results from experiment and modeling - frequency in GHz and  $Q_L$  (in parenthesis) of modes in lowest pass band.

To reach the designed accelerating gradient (50MV/m), the klystron output pulse is to be compressed to higher peak power before injection into the linac. During pulse compression, the RF pulse is manipulated and transmitted over substantial lengths at which copper loss can be significant if it were to remain in the  $TE_{10}$  mode of the klystron output waveguide. A mode transducer has been designed to mode convert to low-loss  $TE_{01}$  mode in overmoded circular guide. Presently in use, the device satisfies the requirements on bandwidth, mode purity and breakdown limit [12]. Figure 5a shows the mode transducer as modeled by HFSS and Fig. 5b shows the input characteristics when compared with experiment. Although exact quantitative agreement was not always possible because the device is sensitive to small dimensional differences, the qualitative results have nevertheless been useful for mode contamination studies.



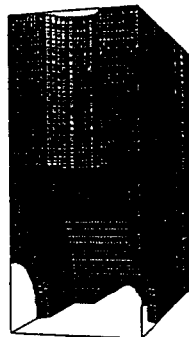
(a)



(b)

Fig. 5 (a) HFSS model of mode transducer without bifurcation (half geometry) and (b) input characteristics from HFSS and experiment.

The RF power coming out of the pulse compression has to be matched into the linac through coupler cavities. Figure 4a shows a symmetric double-input coupler designed to reduce field asymmetry both in amplitude and phase [13]. This coupler has been incorporated into a 30 cm section and operated up to 100 MV/m without breakdown. Figure 4b shows the transmission data comparing MAFIA with measurement [14]. Similar couplers are being designed for the 75cm and 1.8m accelerator sections and computer modeling is playing an important role in determining the matching and tuning of these cavities.



(a)

Standard Cell				
	$\phi$	$f(\text{GHz})$	$Q$	$r(\text{M}\Omega/\text{m})$
m=0	120°	11.425	7261	84.3
m=1	160°	15.146		

2 Pairs of Pumping Holes				
	$\phi$	$f(\text{GHz})$	$Q$	$r(\text{M}\Omega/\text{m})$
m=0	120°	11.425	7283	84.5
m=1	160°	15.145		

(b)

Fig. 6 (a) MAFIA model of pumping cell in detuned structure and (b) tuning results from MAFIA ( $\phi$  is phase advance and  $r$  is shunt impedance).

Inside the NLC linac, the high-power RF pulse will accelerate long trains of  $e^+$  or  $e^-$  bunches. To suppress multi-bunch beam breakup, two schemes have been proposed to heavily damp the wakefields induced by the bunch trains. One is a HOM damping scheme to couple the wakefields out to external loads through waveguides (as in the PEP-II cavity). Damped structure for the NLC was an area of intense activities [15]. Another scheme which is being adopted for the NLCTA is to detune the cells in a systematic way so as to decohere and hence damp the wakefields. Although the individual cells have varying dimensions, the detuned structure is essentially cylindrically symmetric except for the few cells that also serve as vacuum pumping cells. We have modeled these cells to determine their dimensions so they would retain the original accelerating and dipole mode frequencies in spite of the pumping slots. Figure 7a shows one such cell while Fig. 7b shows the tuning results. In this case, reducing the cell diameter by 3.3 microinches allows us to correct for the frequency shifts in the accelerating and dipole modes due to the slot perturbations.

(ii) PEP-II RF Cavity

A considerable amount of modeling effort has been devoted to the design of the PEP-II HOM damped cavity. The two important features of this cavity are: (a) the waveguide damping scheme to reduce HOM impedances, and (b) the thermal/mechanical design to cope with high power dissipation (150 kW on the cavity walls). A low-power test cavity has been constructed for HOM damping studies. Figure 6a shows the mode spectrum without and with damping waveguides. One sees that essentially all the higher-order modes are damped while the accelerating mode at 476 MHz is practically unchanged. Using the MAFIA model shown in Fig. 3a and the Kroll-Yu method, we calculated a  $Q_L$  of 26 for the most dangerous  $TM_{011}$  mode as compared with 28 from measurement. The longitudinal fields on axis of the accelerating mode as found from MAFIA and from bead-pull experiment are compared in Fig. 3b which shows good agreement. The field asymmetry is due to the presence of the damping waveguides.

In designing the cooling system for the cavity, power loss data on the cavity wall has to be generated and input into a mechanical code for thermal stress analysis. Figure 6b shows the distribution of the power dissipated. High power loss is seen around the cavity-waveguide junction and more elaborate cooling is planned for this region. The ongoing mechanical design will be tested in the high-power cavity which is scheduled to go to construction fairly soon. In addition to thermal calculations, the MAFIA model is also heavily utilized in the design of the various coupling networks being considered for the cavity.

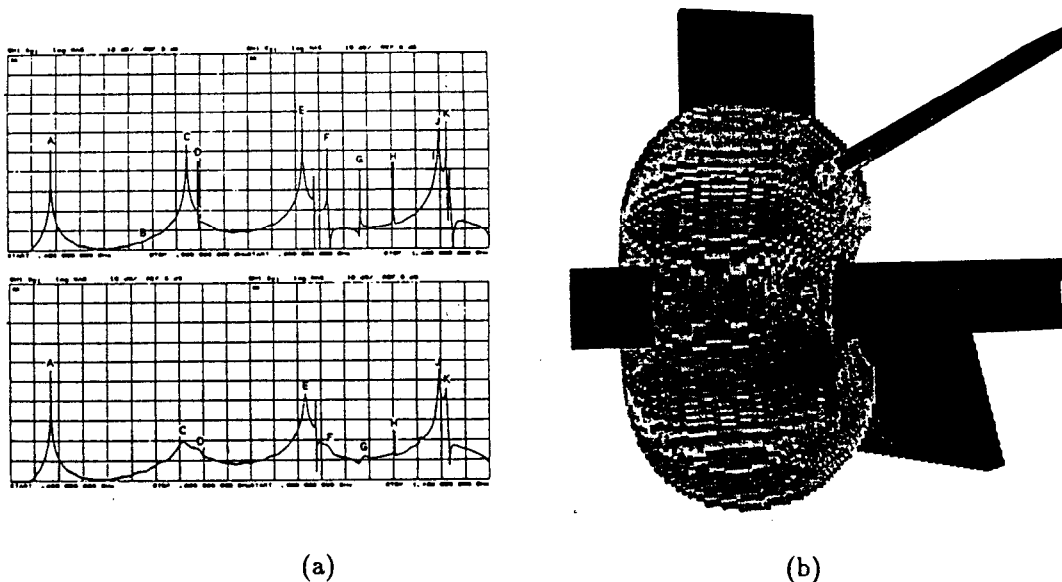


Fig. 7 (a) Modes measured from 0.4-1.4 GHz without damping (top) and with damping (bottom) and (b) power loss on cavity wall (lighter shade indicates higher dissipation).

## 6. CONCLUSION

We have presented an overview of the present status in modeling accelerator structures and RF components. The latest in modeling resources is described and our modeling approach and emphasis explained. The properties of 3D cavities and structures are defined in terms of mode character and external coupling. We have included selected examples from the NLCTA and the PEP-II projects at SLAC to illustrate our principles of application.

## ACKNOWLEDGEMENTS

This paper in essence represents the collective efforts of many individuals from the Numerical Modeling group, the Structures group, the Pulse Compression group and the Klystron department and to them we owe our thanks. We also acknowledge the LBL RF group on the PEP-II collaboration. The help from Thomas Weiland and his group on MAFIA 3.1 as well as the effort of Guy Lemeur on ANTIGONE are appreciated.

## REFERENCES

- [1] R. D. Ruth, 'The Development of the Next Linear Collider at SLAC', *Proc. of Workshop on Physics and Experiments with Linear Colliders*, Saariselka, Finland, September 9-14, 1991; also in SLAC-PUB-5729.
- [2] An Asymmetric B Factory, Conceptual Design Report, LBL-PUB-5303, SLAC-372 (1991).
- [3] R. D. Ruth et. al., 'The Next Linear Collider Test Accelerator', presented at the Particle Accelerator Conference, Washington, DC, May 17-20, 1993; also in SLAC-PUB-6252.
- [4] R. Rimmer et. al., 'An RF cavity for the B Factory', *Proc. of Particle Accelerator Conference*, San Francisco, CA, May 6-9, 1991; also in SLAC-PUB-6129.
- [5] H. K. Deavon and K. C. D. Chan, Eds., 'Computer Codes for Particle Accelerator Design and Analysis: A Compendium', Los Alamos Accelerator Code Group, LA-UR-90-1766, 1990.
- [6] K. Ko, 'Computer Codes for RF Cavity Design', *Proc. of LINAC 92*, Ottawa, Canada, August 24-28, 1992; also in SLAC-PUB-5888.
- [7] N. M. Kroll and D. U. L. Yu, 'Computer Determination of the External Q and Resonant Frequency of Waveguide Loaded Cavities', *Particle Accelerators*, 34, 231 (1990).
- [8] N. M. Kroll and X.-T. Lin, 'Computer Determinations of the Properties of Waveguide Loaded Cavities', *Proc. of Linear Accelerator Conference*, Albuquerque, NM, September 10-14, 1990; also in SLAC-PUB-5345.
- [9] N. M. Kroll, J.-S. Kim and D. U. L. Yu, 'Computer Determination of the Scattering Matrix Properties of N Port Cavities', *Proc. of LINAC 92*, Ottawa, Canada, August 12-18, 1992; also in SLAC-PUB-5880.
- [10] P. Arcioni, 'POPBCI - A Post-Processor for Calculating Beam Coupling Impedances in Heavily Damped Accelerating Cavities', SLAC-PUB-5444, 1991.
- [11] K. Ko, T. G. Lee and N. M. Kroll, 'A Three Gap Klystron Output Cavity at X Band', *Proc. of SPIE's Optics, Electro-Optics and Laser Applications in Science and Engineering Symp.*, Los Angeles, CA, January 19-25 1992; also in SLAC-PUB-5760.
- [12] S. Tantawi, K. Ko and N. Kroll, 'Numerical Design and Analysis of a Compact  $TE_{10}$  to  $TE_{01}$  Mode Transducer', these proceedings.
- [13] G. A. Loew and R. B. Neal, 'Accelerator Structures', in *Linear Accelerators*, p39-133, ed. P. M. Lapostolle and A. L. Septier, 1970.
- [14] C.-K. Ng and K. Ko, 'Numerical Simulations of Input and Output Couplers for Linear Accelerator Structures', these proceedings.
- [15] H. Deruyter et. al., 'Damped and Detuned Accelerator Structures', *Proc. of 1990 Linear Accelerator Conf.*, Albuquerque, NM, September 10-14, 1990; also in SLAC-PUB-5322.